Experimental Investigation of the Effect of Biodiesel Utilization on Lubricating Oil Degradation and Wear of a Transportation CIDI Engine

Shailendra Sinha

Avinash Kumar Agarwal
e-mail: akag@iitk.ac.in

Department of Mechanical Engineering,
Engine Research Laboratory,
Indian Institute of Technology Kanpur,
Kanpur 208016, India

In the present experimental research work, rice-bran oil methyl ester (ROME) is derived through transesterification of rice-bran oil using methanol in the presence of sodium hydroxide catalyst. On the basis of previous research for performance, emission, and combustion characteristics, a 20% (v/v) blend of ROME (B20) was selected as optimum biodiesel blend. This experimental investigation was aimed to investigate the effect of biodiesel on wear of in-cylinder engine components. Endurance tests were conducted on a medium duty direct injection transportation diesel engine with B20. Tests were conducted under predetermined loading cycles in two phases: engine operating on mineral diesel (B00) and engine fueled with B20. After completion of these tests, engines were dismantled for observing the physical condition of various vital engine parts, e.g., piston rings, bearings, cylinder liner, and cylinder head. Physical measurements of these vital parts were also carried out to assess the wear of these parts. The physical wear of various parts except big end bearings (connecting rod bearing bore) were found to be lower in the case of B20 fueled engine. Wear metals in the lubricating oil samples drawn from the engines at regular intervals were investigated. Relatively lower wear concentrations of all wear metals except lead were found in the lubricating oil of B20 fueled engine. To quantify the wear of cylinder liners, surface parameters at different locations in the liner (top dead center, bottom dead center, and midstroke) were measured and compared. A qualitative analysis was also carried out by conducting surface profiles and scanning electron microscopy at the same locations. [DOI: 10.1115/1.3077659]

1 Introduction

The increasing industrialization and motorization of the world has led to a steep rise in demand for petroleum products, which has led to the twin crises of fossil fuel depletion and environmental degradation [1].

Compared with the rest of the world, India's demand for diesel fuels is roughly five times that of gasoline (8 MMT Petrol demand versus 40 MMT diesel demand in 2005–2006) [2]. In 2005–2006, consumption of crude oil increased to approximately 130 MMT, and more than 75% of it was imported. Import bill has increased substantially during the past two decades (U.S.$ 1.36 billion in 1991 to U.S.$ 38.1 billion in 2005–2006), which constituted 37% of the net export earnings [3]. Therefore, the issue of utilization of biofuels especially in diesel engines is very important for India.

Vegetable oils have about 90% heat content of mineral diesel and their combustion related properties are somewhat similar to mineral diesel [4–8]. However, several properties of oils, such as high viscosity, high molecular weight, and low volatility, cause poor fuel atomization leading to incomplete combustion resulting in problems such as severe engine deposits, injector coking, and piston ring sticking [8–16]. Hence straight vegetable oils are not suitable for use in engines; they need to be modified to bring them closer to mineral diesel in their properties. Among the various fuel modification techniques available (e.g., pyrolysis, blending, microemulsion, and transesterification), transesterification is the most effective and widely used technique for modifying properties of vegetable oils [8,9,17–23]. Transesterification is a well established chemical reaction in which alcohol reacts with triglycerides of fatty acids in the presence of a catalyst. It is a reversible reaction of fat or oil with a primary alcohol in which alcohol combines with the triglycerides to form 1 mole of glycerol and 3 moles of monoalkyl esters, molar mass of which is approximately one-third of triglycerides [8,9,18–20,23–25]. The monoalkyl esters thus produced are commonly known as biodiesel. Biodiesel is biodegradable, nontoxic, essentially sulfur-free, renewable fuel and can be produced from agriculture and plant resources available locally. In the case of spill in the environment, biodiesel degrades four times faster than mineral diesel and the carbon cycle time for fixation of CO_2 from biodiesel is quite small compared with mineral diesel [26,27]. In addition, biodiesel lowers exhaust emissions compared with mineral diesel. In the previous study in our laboratory [28,29] with rice-bran biodiesel, it was found that HC and CO emissions reduce drastically with a small increase in the NO_x emission as compared with mineral diesel. Marginally higher NO_x emission is due to the early start of combustion, due to the higher cetane number of biodiesel, which acts to advance start of combustion. It can be reduced by retarding the injection timing. Biodiesel provides significant fuel lubricity properties. Biodiesel may also be added to low sulfur mineral diesel in order to compensate for loss of lubricity due to the removal of sulfur compounds [30–32].

The effect of fuel on wear of engine components is very important as it affects the engine durability, fuel economy, and emissions. The main causes of wear are metal-to-metal contact, the presence of abrasive particles, and attack by corrosive acids

Manuscript received June 10, 2007; final manuscript received October 20, 2008; published online January 12, 2010. Review conducted by Dilip R. Ballal. Paper presented at the 2007 Fall Conference of the ASME Internal Combustion Engine Division (ICEF 2007), Charleston, SC, October 14–17, 2007.

Copyright © 2010 by ASME

Downloaded 02 Jun 2010 to 171.66.16.96. Redistribution subject to ASME license or copyright; see http://www.asme.org/terms/Terms_Use.cfm

formed during the combustion process. The lubricant transports protective chemicals to the sites where they are needed and transports waste products away from the sites where they are generated [33]. Several researchers reported that soot is one of the main factors that increases engine wear as it interacts with oil additives and reduces the effectiveness of antiwear additives [34–37]. This results in breakdown of the oil film permitting contact between soot particles and the engine surfaces. Under these conditions, the lubricant boundary layer is about 0.001-0.05 μm thick. However, soot particles have diameters ranging from 0.01 μm to 0.8 μm and could therefore cause abrasive wear. Boundary lubrication occurs at top dead center (TDC) and bottom dead center (BDC) positions of the cycle and hence, maximum wear occurs at these positions [34,38].

Cylinder liner wear mainly corresponds to wear of the surface topography in the peak and core zones. The valley zone is less affected. Surface wear at TDC and BDC locations is more severe than at the middle [39]. Atomic absorption spectroscopy (AAS) is one of the most commonly used techniques for qualitative and quantitative analysis of wear debris in lubricating oil [23,40–43].

Peterson et al. reported 1000 h EMA engine test with three identical engines fueled with 100%, 50%, and 25% blends of hydrogenated soy ethyl ester (HySEE) and observed lower wear and cleaner internal engine parts with 100% HySEE. Kaufman and Ziejewski [44] conducted 200 h EMA durability test with sunflower methyl ester as a fuel on turbocharged intercooled DI engine and compare it with base line mineral diesel data. Initial and final measurements on engine did not indicate any significant wear, less carbon buildup in the intake ports, intake valve tulips, and comparable carbon buildup in the exhaust port with methyl ester. Slightly more carbon deposits were observed on the valve stems and on the cylinder sleeves above the ring travel area and piston top land for methyl ester fuel. Clark et al. [12] reported comparable deposits on engine parts, however, slightly different in color and texture, with the methyl ester engine experiencing greater carbon and varnish deposits on the pistons. The physical measurements and inspection showed no noticeable difference. No wear was measurable on the cylinder walls (liners) and pistons, and no rings were found stuck in the grooves. In all cases, the original honing marks in the liners were clearly visible. Slightly higher levels of aluminum and lead in lubricating oil were reported with methyl ester. Kalam and Masjuki [42] performed 100 h test with half throttle setting at constant speed (2000 rpm) for different blends of palm oil methyl ester containing anticorrosion additive and observed lower wear with 15% blend of palm oil methyl ester. Fraer et al. [45] reported higher sludge formation (enriched in sodium) on the valve deck around the rocker assemblies and more injector replacement for B20 fueled engine (over 60,000 mile operation) particularly for Mack tractor engines. Kenneth et al. [46] reported the results for nine identical transit buses (five operated on B20 and four on mineral diesel) for a period of 2 years (about 100,000 miles). They observed occasional fuel filter plugging for the B20-fueled buses, no additional wear metals from the use of B20, similar rates of TBN and ZDDP decay for B20 and mineral diesel, and significantly lower soot levels for the B20 vehicles during lubricating oil analysis. Agarwal et al. [23,43] found less carbon deposits and lower wear ($\approx$30% lower) of engine parts in the case of 20% linseed oil methyl ester fueled engine during endurance test on a constant speed DI diesel engine.

2 Fuel Preparation and Characterization

Rice-bran oil is obtained from the outer brown layer of rice called rice-bran. Rice-bran oil is considered to be edible and nonedible. Oil extracted from bran may have low or high acidity, depending on the conditions and duration of storage. India is the second largest producer of rice (about 22% of the world) in the world, next to China. India has a potential to produce about 1×10^6 tonnes of rice-bran oil per annum. Fatty acid composition of rice-bran oil as reported in literature is shown in Table 1.

Table 1 Fatty acid composition of rice bran oil [8,47]

Fatty acid	Molecular weight	Srivastava et al. [8]	Zullaikah et al. [47]
Myristic (14:0)	228	0.4–0.6	0.21 ± 0.1
Palmitic (16:0)	256	11.7–16.5	14.7 ± 0.47
Stearic (18:0)	284	1.7–2.5	1.86 ± 0.22
Oleic (18:1)	282	39.2–43.7	42.2 ± 0.68
Linoleic (18:2)	280	26.4–35.1	37.8 ± 0.51
Linolenic (18:3)	278	-	2.39 ± 0.1
Arachidic (20:0)	312	0.4–0.6	n.d.
Behenic (22:0)	340	-	0.2 ± 0.1
Lignoceric (24:0)	368	0.4–0.9	0.3 ± 0.14

Rice-bran oil was transesterified, using methanol in the presence of NaOH catalyst. Process parameters such as temperature, catalyst amount, molar ratio of alcohol to oil, and reaction temperature were optimized and these were 9:1 molar ratio of alcohol to oil, 55°C temperature, 0.75% (w/w) catalyst, and 1 h reaction time for transesterification of rice-bran oil in our laboratory [48]. The blends of biodiesel are referred as Bxx, where xx refers the percentage of ester by volume (v/v) in that blend. Characterization of rice-bran oil, ROME, and diesel were done in laboratory as per ASTM standards. Some fuel properties evaluated are shown in Table 2.

3 Experimental Setup and Methodology

A typical medium duty transportation compression ignition direct injection (CIDI) engine (Mahindra & Mahindra Ltd., India, Model: MDI-3000) was used for conducting engine investigations. The specifications of the engine are given in Table 3.

The inlet valve opens 5° BTDC and closes 35° ABDC. The exhaust valve opens 42° BBDC and closes 10° ATDC. The engine was coupled with eddy current dynamometer and controller (Schenck Avery, India; Model: ASE 70). The suitable instrumentation was done for conducting various experiments. Engine speed

Table 2 Properties of fuels

Property		Test method	Diesel	ROME
Specific gravity at 30°C			0.839	0.877
Viscosity (cS) at 40°C		ASTM D445	3.18	5.29
Cetane No.		ASTM D613	51	63.8
Cloud point/pour point (°C)		ASTM D2500	6/−7	9/−2
Flash point/fire point (°C)		ASTM D93	68/103	183/196
Calorific value (MJ/kg)		ASTM D 240	44.8	42.2
Elemental analysis (% w/w)	C		83	72.96
	H		13	12.73
	N		1.76	0.94
	O		0.19	11.59
	S		0.25	n.d.

Table 3 Specification of the test engine

Manufacturer/model	M&M Ltd., India/MDI 3000
Engine type	Four stroke, naturally aspirated, water cooled diesel engine
Number of cylinders	Four
Combustion system	Direct injection, re-entrant bowl
Bore/stroke	88.9/101.6 mm
Displacement volume	2520 cc
Compression ratio	1 8:1
Cylinder liners	Cast iron replaceable wet liner
Start of fuel injection	$15 \pm 1°$ BTDC
Rated power	55 hp at 3000 rpm
Max. torque	152 Nm at 1800 rpm

Downloaded 02 Jun 2010 to 171.66.16.96. Redistribution subject to ASME license or copyright; see http://www.asme.org/terms/Terms_Use.cfm

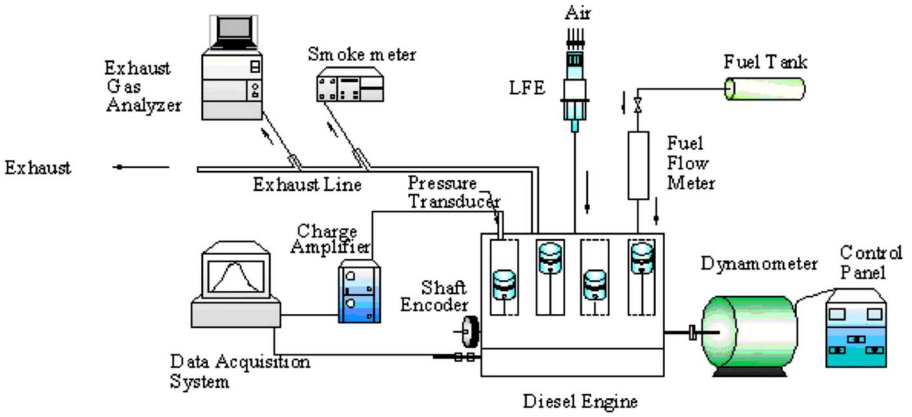

Fig. 1 Schematic of experimental setup

and load were controlled by varying excitation current to the eddy current dynamometer. The schematic of experimental setup is shown in Fig. 1. After conducting performance and emission, investigations at full fuel delivery settings and different engine speeds [28,29], 20% blend of rice-bran biodiesel (B20) was found to be optimum blend (superior thermal efficiency and lower emission) and selected for long-term endurance test. The long-term engine endurance experiments were conducted in two phases. In the first phase, the engine was run with diesel (B00), and in the second phase, the engine was run with B20. The engine was initially dismantled and a new set of cylinder liners, pistons, piston rings, and bearings were used for conducting experiments for each of the two phases.

After physical examination, dimensions of various parts such as cylinder head, cylinder bore/liners, pistons, piston rings, gudgeon pin, small end bush, big end bearings, and weight of piston rings were recorded. The engine was subjected to 10 h duration preliminary run before commencing the endurance test. This was done according to test procedure given in IS: 10000 part V, 1980 [49]. After a preliminary run, the lubricating oil from the sump was drained off and the engine was refilled with fresh lubricating oil (SAE 20W40), as specified by the manufacturer, and the engine was then ready for long-term endurance test. The endurance test was performed as per Indian standard code (IS: 10000 Part IX, 1980) [50].

The test was conducted for a total of 100 h duration and consists of ten nonstop running cycles of 10 h duration each. Each running cycle consists of five repetitive runs of 2 h duration each (Table 4). The lubricating oil samples were collected from the engine after every 20 h for wear metal analysis.

After conducting the endurance test for the first phase, the engine was again dismantled and the physical condition of various engine components was inspected carefully. The dimensions of critical parts and weight of piston rings were recorded. Carbon deposits on various engine components were photographed and physical measurement of components listed earlier were made carefully. Wear was estimated by accurate measurement of dimensions of various vital parts mentioned earlier before and after endurance test. The cylinder head and injectors were cleaned thoroughly to remove the carbon deposits. The engine was reassembled with new set of cylinder liners, piston, piston rings, and big end bearings for conducting the endurance test on the same engine while operating with B20. The similar procedure, i.e., preliminary runs, endurance test, lubricating oil collection, and wear measurement, was followed for second phase (B20) also. Lubricating oil samples were analyzed on a flame AAS (GBC, Australia; Model: Avanta Σ) for evaluating the metallic composition of wear debris. The cylinder liner surface profile was evaluated for various surface characteristics before and after completion of each phase. The surface profiles of the cylinder liner surfaces were taken using stylus based surface profilometer (Mitutoyo, Japan; Model: SJ-301). The surface roughness is determined from the vertical stylus displacement produced during the stylus traverse over the surface irregularities. In wear analysis, scanning electron microscopy (SEM) is a natural extension of optical microscopy. The wear of cylinder liner surfaces was compared by SEM after 100 h endurance test. The magnification used was kept at 150×. The SEM micrographs were taken at three locations (TDC, midstroke, and BDC) on both thrust side and antithrust side for both sets of experiments for assessing comparative wear.

Table 4 Engine loading cycle for endurance test [50]

Engine speed	Load (% of rated load)	Running time (min)
Maximum speed	75	50
Maximum torque speed	100	45
Idling	No load	5
Maximum speed	100	20

4 Results and Discussions

4.1 Comparison of Carbon Deposits on Vital In-Cylinder Engine Parts. Diesel engines have several critical components working under close tolerances, which are subjected to high temperatures and mechanical stresses. Deposits on these components generally originate due to the thermal and oxidative degradation of lubricants and pyrolysis/incomplete combustion. These deposits degrade engine performance, efficiency, and cause operational problems and also increase maintenance. Sometimes heavy deposits may also lead to engine failure. A qualitative analysis of carbon deposits on various vital engine parts was done (photographically). The engine power output was kept constant during endurance test, i.e., engine was running at the similar speed and load conditions for both phases of the experiment. Photographs of various in-cylinder engine parts, namely, cylinder head, piston crown, and injector tip, were taken for both phases before and after the endurance test, in order to compare soot formation/carbon deposits on these parts.

The physical conditions of various vital engine components directly exposed to combustion (after endurance test) are shown in the Fig. 2. It can be clearly seen from these photographs that carbon deposits on the cylinder head, injector tip, and piston crown of biodiesel fueled engine is significantly lower compared with mineral diesel fueled engine.

Less carbon deposits on cylinder head, injector tip, and piston crown of biodiesel fueled engine confirm that the main hurdle in

Downloaded 02 Jun 2010 to 171.66.16.96. Redistribution subject to ASME license or copyright; see http://www.asme.org/terms/Terms_Use.cfm

Fig. 2 Carbon deposits on vital engine parts

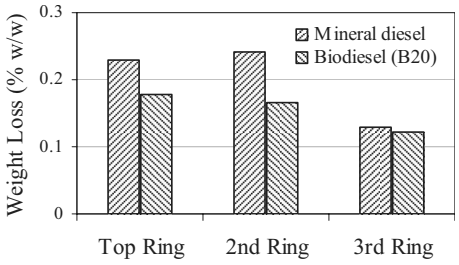

Fig. 3 Percent weight loss of piston rings after 100 h of engine operation

utilizing straight vegetable oils/blends, i.e., large carbon deposits and coking of injector tip, disappeared after the transesterification of vegetable oils. Lower carbon deposits on these components may be due to the lower soot formation during the combustion of biodiesel in the engine. This observation can also be correlated with a similar pattern observed while conducting exhaust smoke opacity measurements on the same engine operating on different blends of biodiesel and mineral diesel (during performance and emission investigations conducted earlier) [28] and also by Kenneth et al. [46]. This improved combustion and lower soot formation in the case of biodiesel is due to the presence of oxygen in the fuel molecule. Oxygenated fuels are known to produce lower soot and particulate formation during combustion in diesel engines.

4.2 Wear Measurement of Vital Parts. The relative motion of engine parts lead to wear of moving surfaces in contact. Engine was operated under identical load/speed conditions for both fuels; hence the effect of new fuel on engine components could be compared directly and material compatibility of new fuel vis-a-vis mineral diesel can also be judged. The wear of these parts during endurance test was estimated by accurate measurement of physical dimensions of various vital parts before the commencement and after the completion of endurance test. The wear of different engine components for both the fuels is shown in Appendix (Tables 7–12). Wear in valve seat is measured by a reduction in the distance of valve head from mounting flange face (Table 7). Lower wear (12–35%) was observed in the case of biodiesel fueled engine. Piston dimensions were taken at the three locations (Table 8). Wear of piston was found to be in the range of 0.01–0.08 mm for engine operating on both fuels. Generally relatively lower wear was observed for biodiesel fueled engine. Measurements of connecting rod bearing bore before and after the endurance test was done (Table 9) for mineral diesel and biodiesel fueled engines. Some measurements show higher wear for biodiesel and some for mineral diesel. No definite conclusion can be drawn. Marginally higher wear was observed for biodiesel fueled engine. Wear of gudgeon pin, pin bore, and small end bush are comparable for both sets of experiment (Table 11).

Piston rings are subjected to high thrust imposed by combustion gases. In the present setup, piston ring pack consists of three rings: two compression ring and an oil control ring. Top ring face was chrome plated to reduce the wear due to the abrasive and corrosive conditions prevailing in combustion chamber. For assessing the wear of piston rings, piston rings axial width (H1), radial wall thickness (A1), and ring gap (S1) (Table 10) were measured. Generally lower wear was observed for the biodiesel fueled engine. The wear was found to be very low (<0.02 mm) and it was very difficult to compare the results of the measurements taken by micrometer of 0.01 mm accuracy; thus for more accurate wear determination of piston rings, weight loss of rings was also analyzed for both sets of experiments. The percentage weight loss of piston rings for both phase of experiments are shown in Fig. 3. It was observed that second compression ring had maximum weight loss and oil control ring had the minimum weight loss for engine operating on mineral diesel and biodiesel. In the case of B20 fueled engine, lower weight losses ($\approx$35%) for compression rings and for oil control ring ($\approx$12%) were observed. This may be possibly due to the improved biodiesel combustion, lower peak in-cylinder temperature, less soot formation, and better inherent lubricity properties of biodiesel.

Wear of cylinder liner was measured along the crank shaft axis and perpendicular to the crank shaft axis at five locations (Table 12). For both phases, wear was found to be higher in the direction perpendicular to crank shaft axis. This may be due to the acting thrust on the piston and piston tilt during the stroke. Wear of the liner was found to be extremely low (<0.01 mm) and it is not justified to compare the readings taken by the bore gauge of 0.01 mm least count.

4.3 Wear Metal Analysis of Lubricating Oil. Wear debris originate from various sliding and rotating components in engine and are washed away by lubricants and finally get accumulated in the oil sump. Various metals such as Fe, Cu, Cr, Al, Ni, Zn, Mg, and Pb were analyzed in the lubricating oil samples drawn at regular intervals from both phases of experiment. Each of these metals can be traced back to several engine components. Typical sources of wear metals present in the lubricating oil are shown in Table 5. For extraction of heavy metals from the lubricating oil, dry ashing technique was used [40]. The lubricating oil ash was dissolved in concentrated aqua-razia and mixture was diluted by distilled water, and then analyzed thrice on AAS; the average value of these readings is reported in Fig. 4. This figure shows an increasing trend of metallic concentration in the lubricating oil with its usage. Metallic concentration rises at a faster rate initially followed by slow and steady rise later for both phases of the experiment. The reason for this behavior may be higher wear rate due to the initial running-in of newer in-cylinder engine components.

Figure 4(*b*) shows the concentration of zinc as a function of lubricating oil usage. Zinc containing compound ZDDP is added

Downloaded 02 Jun 2010 to 171.66.16.96. Redistribution subject to ASME license or copyright; see http://www.asme.org/terms/Terms_Use.cfm

Table 5 Typical sources of wear metals in lubricating oil

Element	Typical sources
Aluminum (Al)	Piston, bearing, dirt
Chromium (Cr)	Compression rings, coolant, crankshaft, gears, bearings, plating of cylinder liner
Copper (Cu)	Bearings, bronze bushings
Iron (Fe)	Cylinder liner, piston, rings, valves, gears, shafts, antifriction bearings, crankshaft
Lead (Pb)	Bearings, grease paint
Magnesium (Mg)	Bearings, additives, supercharger, gearbox
Nickel (Ni)	Bearings, valves, gear plating, additives
Zinc (Zn)	Additives, bearings, plating, brass components, neoprene seals

to the lubricating oil as multifunctional additive such as antioxidant, antiwear additive, detergent, and extreme pressure additive. Fresh lubricating oil contains a reasonable amount of zinc as organometallic complex. The presence of zinc in used lubricating oil may be because of additive depletion, wear of bearing, brass components, and neoprene seals. Kalam and Masjuki [42] reported a continuous decrease in Zn while Agarwal et al. [23,43] reported an increase in zinc concentration with the usage of lubricating oil. In the present investigation, it has been found that concentration of zinc in the lubricating oil gets reduced during initial hours of engine operation but after 20 h, the concentration rises for both phases of the experiment. A similar trend is also reported by Zieba-Palus [40] for diesel engines. The reduction in zinc concentration for the initial period may be because of evaporation of zinc containing species from the lubricating oil due to the initial thermal stressing of lubricant. Afterwards, zinc gets added to lubricating oil due to the wear of various engine parts, thus increasing the concentration of zinc in lubricating oil continuously.

Concentration of lead is observed to be lower for the biodiesel fueled engine up to 70 h of engine operation; however, afterwards it becomes higher for the B20 fueled engine. Staat and Paul [51] and Clark et al. [12] also reported higher lead concentration in the used lubricating oil of biodiesel fueled engine.

This may be due to the action of biodiesel on the paint of different engine components or slightly more wear taking place on bearings (found during physical measurement). This is in agreement with the findings of Clark et al. [12]. Similar trend is found for aluminum, after 100 h of engine operation, where it becomes higher (≈2%) in B20 fueled engine. This increase is somewhat lower than observed by Clark et al. [12] for soybean esters. The results of AAS for various metals show that lubricating oil samples drawn from biodiesel fueled engine has lower concentration of wear metals, indicating that use of B20 leads to a reduction in wear of the engine components, thus enhancing engine durability.

4.4 Surface Roughness Measurement. Surface profiles of the liners were evaluated at three locations, i.e., TDC, midstroke, and BDC. Profiles were taken for both thrust and antithrust sides before and after the endurance test nearly on the same locations for both sets of experiment. The surface profilometer evaluates the surface texture and gives a number of surface parameters such as R_a, R_q, R_p, and R_v. The evaluation length of the surface profile was kept 4.0 mm. The roughness profile and SEM of fresh liner is

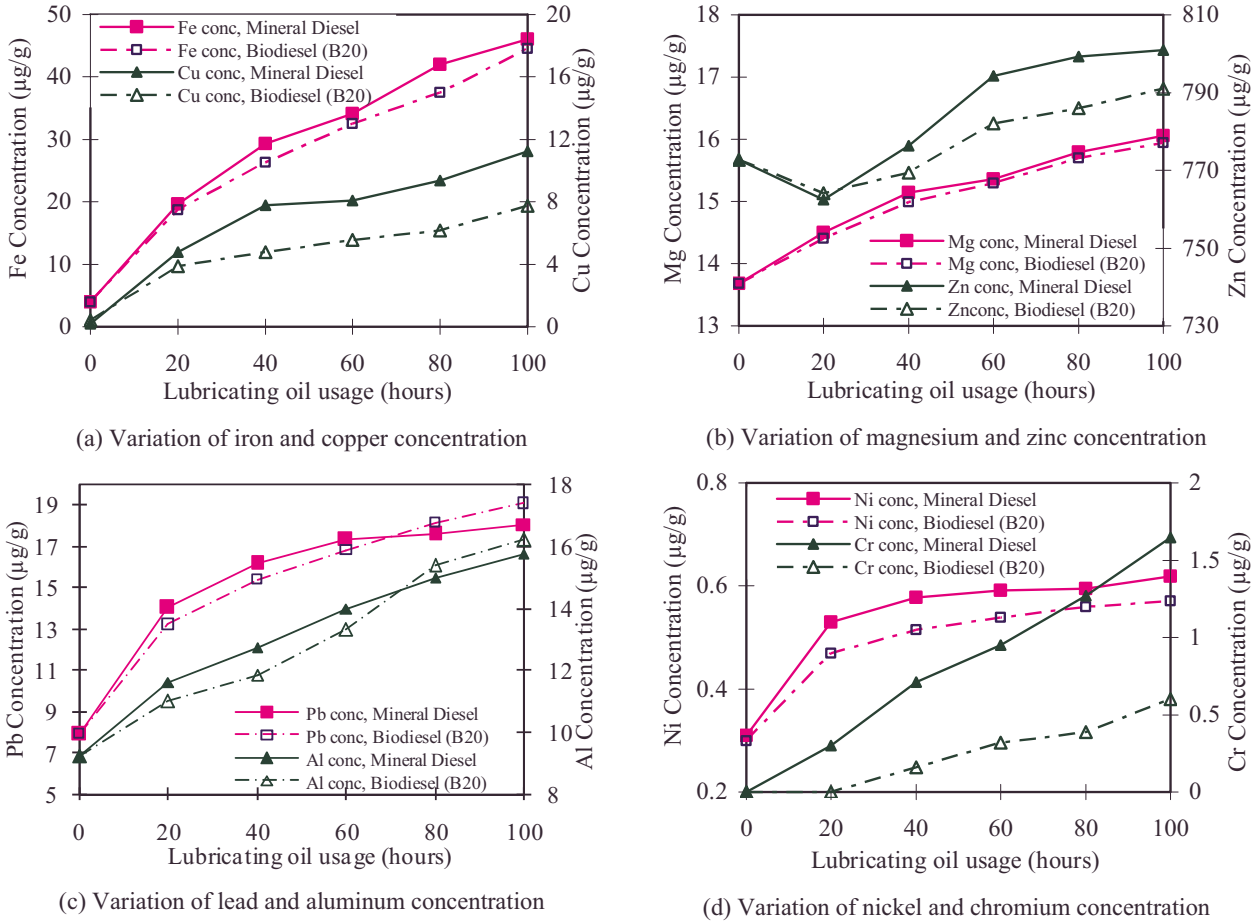

(a) Variation of iron and copper concentration

(b) Variation of magnesium and zinc concentration

(c) Variation of lead and aluminum concentration

(d) Variation of nickel and chromium concentration

Fig. 4 Concentration of wear metals in lubricating oil

Downloaded 02 Jun 2010 to 171.66.16.96. Redistribution subject to ASME license or copyright; see http://www.asme.org/terms/Terms_Use.cfm

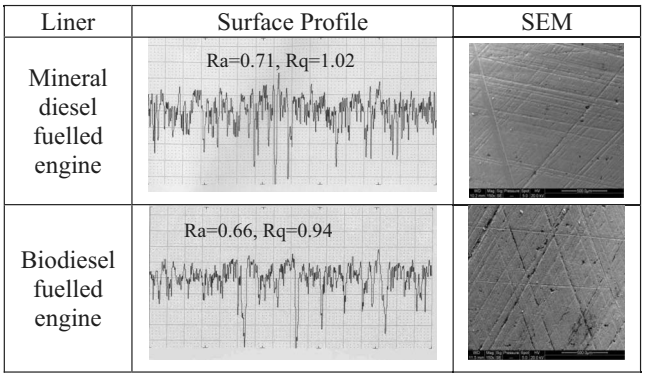

Fig. 5 Surface profiles and SEM of fresh liner surfaces

shown in Fig. 5. The roughness parameters of cylinder liner on thrust and antithrust sides for mineral diesel and biodiesel fueled engine are shown in Table 6 and surface profiles are shown in Fig. 6. From these roughness parameters, it can be observed that the wear of the liner at TDC is higher than BDC and midstroke positions. Change in the most important roughness parameters, i.e., average roughness (R_a) and root mean square roughness (R_q) at TDC, midstroke, and BDC locations have also been calculated. Change in R_a and R_q values is found to be lower at thrust side showing relatively lower wear on the thrust side. Change in R_a and R_q is higher at TDC location indicating maximum wear at the TDC location. The wear found at TDC location is higher because at dead center positions, linear velocity of piston is close to zero and maximum at midstroke position.

At TDC and BDC locations, boundary lubrication takes place, while at midstroke location, hydrodynamic lubrication takes place. Also the TDC zone faces highest temperature and pressure due to the combustion taking place near TDC. Due to these extreme conditions, breakdown of the oil film takes place, leading to relatively higher wear at this location.

4.5 SEM. The wear of cylinder liner surfaces after 100 h endurance test was compared qualitatively by SEM. The magnification used was 150×. The SEM for fresh liners for both set of experiments, before starting the endurance test, was done (Fig. 5). Typical cross-hatched honing marks are clearly visible on both fresh liners. The SEMs of used liner surfaces were also conducted after the endurance test at three locations (TDC, midstroke, and BDC) on both thrust and antithrust sides for both sets of experiment (mineral diesel and biodiesel fueled engine) and shown in Fig. 7. It has been observed that honing depth is not completely removed; however, honing marks become less pronounced as compared with fresh liner for both sets of experiments. These micrographs show very low wear and substantiate the results of physical measurements. Smoother surface (less pronounced cross-hatched marks) indicate higher wear. It can be observed that wear of the liner is higher at TDC positions on both thrust and antithrust sides compared with midstroke and BDC locations. This substantiates the findings of surface roughness profiles. It can also be observed that wear of cylinder liner is higher on the antithrust side compared with thrust side. These wear patterns can be related to the piston motion and tilting position patterns as the piston

Table 6 Roughness parameters of liner surface of mineral diesel and biodiesel fueled engine

Roughness parameters (μm)	Fresh liner			After 100 h endurance test					
				Thrust side			Antithrust side		
	TDC	Midstroke	BDC	TDC	Midstroke	BDC	TDC	Midstroke	BDC
R_a	0.69 (0.65)[a]	0.82(0.74)	0.71(0.66)	0.3(0.44)	0.56(0.59)	0.48(0.51)	0.14(0.19)	0.48(0.45)	0.3(0.36)
R_q	0.91 (0.9)	1.25(1.09)	1.02(0.94)	0.47(0.68)	0.85(0.89)	0.69(0.76)	0.34(0.35)	0.8(0.69)	0.59(0.61)
R_t	5.92 (6.24)	11.19(11.67)	10.47(7.89)	3.67(5.75)	6.54(6.84)	5.55(6.99)	4.78(4.63)	8.14(7.12)	7.35(5.54)
R_p	1.68 (1.76)	2.11(1.75)	2.38(1.85)	0.83(2.04)	1.01(1.27)	0.82(1.63)	0.39(0.69)	1.14(0.86)	0.88(0.65)
R_v	4.24 (4.48)	9.08(9.92)	8.09(6.03)	2.84(3.7)	5.53(5.57)	4.73(5.36)	4.39(3.93)	7.0(6.26)	6.46(4.9)
δR_a	-	-	-	0.39(0.21)	0.18(0.23)	0.23(0.15)	0.55(0.46)	0.26(0.37)	0.41(0.3)
δR_q	-	-	-	0.44(0.22)	0.24(0.36)	0.33(0.18)	0.57(0.55)	0.29(0.56)	0.43(0.33)

[a]The values in the parentheses are for biodiesel fueled engine.

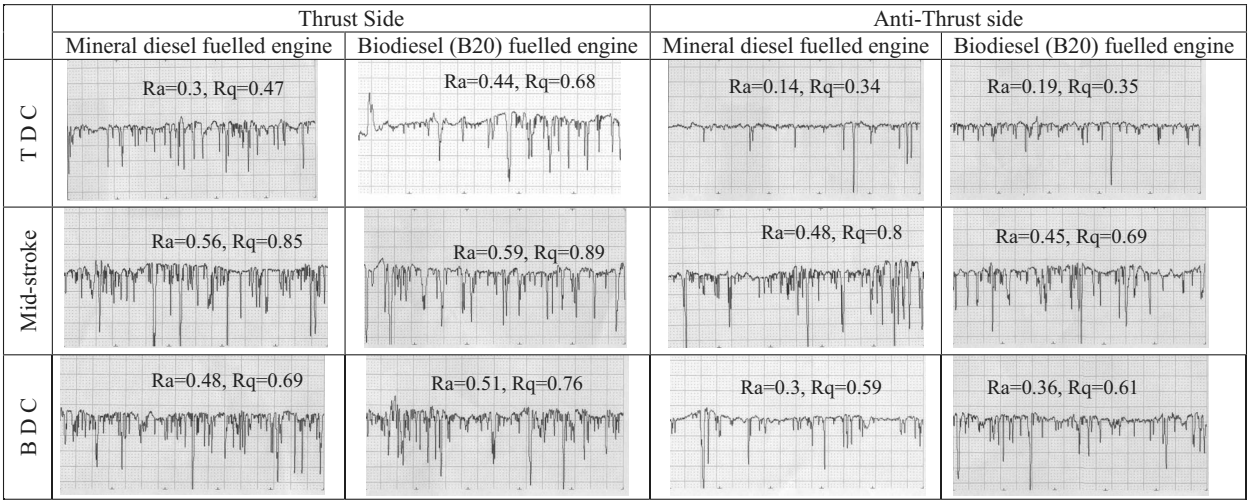

Fig. 6 Surface profiles of liner surface of mineral diesel and biodiesel fueled engine

Downloaded 02 Jun 2010 to 171.66.16.96. Redistribution subject to ASME license or copyright; see http://www.asme.org/terms/Terms_Use.cfm

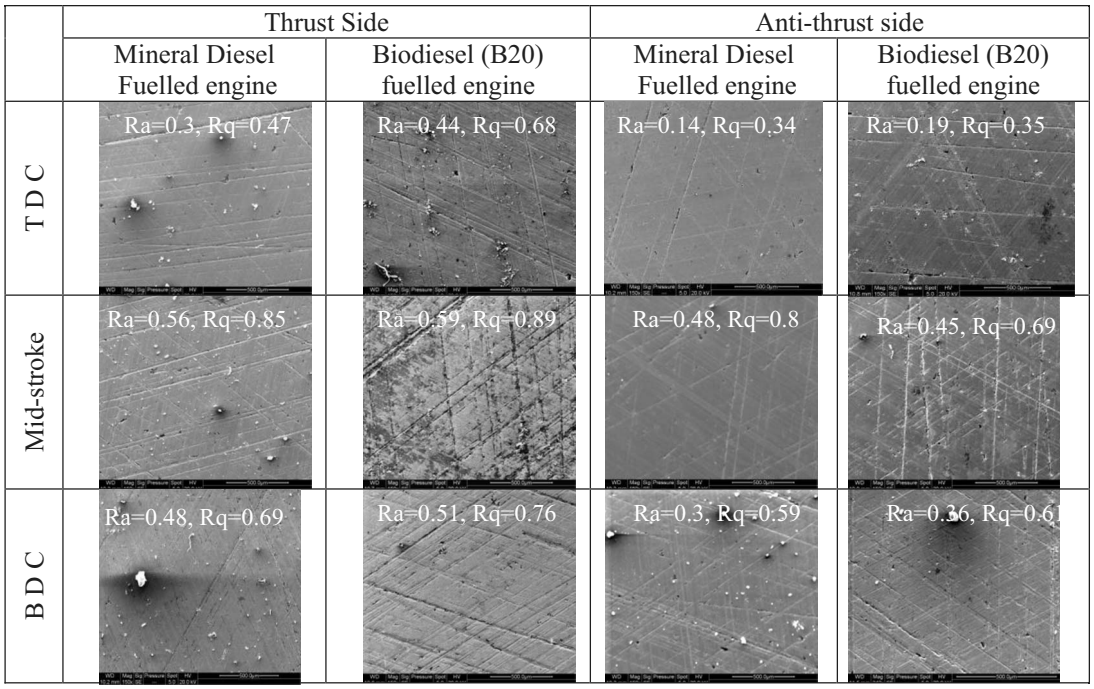

Fig. 7 SEMs of liner surfaces of mineral diesel and biodiesel fueled engine

traverses. It is reported that during four strokes of piston operation, the main contact is on the antithrust side (during the compression, expansion, and exhaust strokes). Contact occurs on the thrust side during the intake stroke only, when cylinder pressure and temperature are both comparatively low [39]. Figure 7 shows that cylinder liner wear in biodiesel fueled engine is comparatively lower (lower damage to cross-hatched honing marks) compared with mineral diesel fueled engine.

5 Conclusions

An endurance test was carried out on the CIDI engine with rice-bran oil biodiesel to see its viability as a substitute for mineral diesel. Less carbon deposits on the in-cylinder parts are observed for 20% biodiesel (B20) blend. Physical measurements of various vital parts show lower wear for biodiesel fueled engine except the big end bearing, which shows slightly higher wear in the case of B20 fueled engine. Less wear was found for piston rings of B20 fueled engine. The second ring wear was found to be higher compared with other rings for both phases of the experiment.

Wear metal analysis in lubricating oil samples further shows lower wear for B20 fueled engine. Pb and Al were found slightly higher for B20 fueled engine, which may be due to the attack of biodiesel on paints and bearings. The wear pattern of cylinder liner surfaces was also analyzed. Very low wear was observed for the cylinder liner and it was difficult to measure using bore gauges. Surface roughness profiles, various roughness parameters, and SEM micrographs show that wear is relatively higher at the antithrust side and at TDC location. Similar wear trend was found with B20 fueled engine but overall wear was lower than diesel fueled engine.

A long-term endurance test conclusively proved that biodiesel can be successfully used for partial substitution of mineral diesel. It can also be concluded that biodiesel can readily be adopted as an alternative fuel in the existing CIDI engines without any major modifications in the engine hardware.

Acknowledgment

The authors acknowledge Mohan Lal Saini and Roshan Lal of Engine Research Laboratory, Department of Mechanical Engineering, IIT Kanpur for their help in conducting engine experiments. Research funding provided by Department of Science and Technology, New Delhi, India for conducting this research is highly acknowledged.

Appendix

Wear of Various Vital Engine Parts for Mineral Diesel and Biodiesel Fueled Engine (Tables 7–12)

Table 7 Measurements of cylinder head

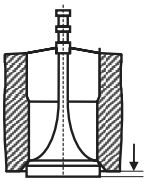

	Distance of valve head from mounting flange face (mm)	
	Wear (mm)	
	Mineral Diesel	Biodiesel
Inlet valve	0.016	0.014
Outlet valve	0.057	0.043

Table 8 Measurements of piston dimensions

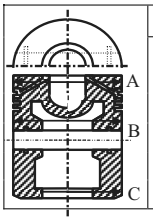

	Diameter of piston at position (mm)	Wear (mm)			
		Mineral Diesel		Biodiesel	
		ϕx	ϕy	ϕx	ϕy
A		0.02	0.01	0.0	0.01
B		0.06	0.02	0.05	0.04
C		0.08	0.07	0.01	0.02

Downloaded 02 Jun 2010 to 171.66.16.96. Redistribution subject to ASME license or copyright; see http://www.asme.org/terms/Terms_Use.cfm

Table 9 Measurements of connecting rod bearing bore

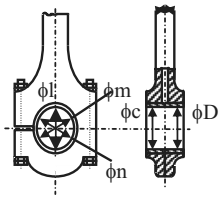

		Wear (mm)	
		Mineral Diesel	Biodiesel
ϕC (mm)	ϕl	0.08	0.08
	ϕm	0.1	0.06
	ϕn	0.02	0.08
ϕD (mm)	ϕl	0.02	0.10
	ϕm	0.04	0.06
	ϕn	0.02	0.06

Table 10 Measurements for piston rings

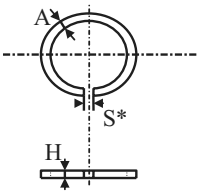

*measured by slip gauges

	Ring No.	Wear (mm)		
		A	H	S*
Mineral Diesel	1	0.01	0.01	0.076
	2	0.01	0.01	0.151
	3	0.01	0.00	0.101
Bio-diesel	1	0.01	0.01	0.051
	2	0.01	0.01	0.127
	3	0.00	0.00	0.051

Table 11 Measurements of gudgeon pin, pin bore, and small end bush of connecting rod

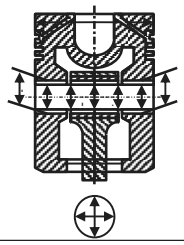

		Wear (mm)						
		Gudgeon pin Bore (in piston)		Gudgeon pin diameter			Small end bush	
		ϕa1	ϕa2	ϕb1	ϕb2	ϕb3	ϕc1	ϕc2
Mineral Diesel	X	0.02	0.02	0.02	0.02	0.04	0.02	0.01
	Y	0.01	0.02	0.04	0.04	0.04	0.01	0.01
Biodiesel	X	0.0	0.02	0.02	0.0	0.0	0.01	0.01
	Y	0.02	0.03	0.01	0.02	0.03	0.01	0.0

Table 12 Measurements of cylinder bore/cylinder liner

From TDC, A= 14 mm, B= 35 mm
C= 5 mm, D= 85 mm, E= 115 mm

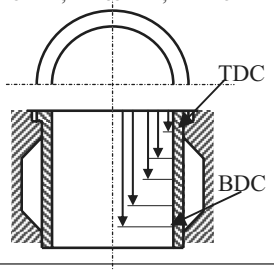

		Wear (mm)				
		A	B	C	D	E
Mineral Diesel	Along crank shaft axis	0.01	0.00	0.00	0.00	0.01
	Perpendicular to crank shaft axis	0.01	0.01	0.01	0.01	0.01
Biodiesel	Along crank shaft axis	0.01	0.00	0.00	0.00	0.00
	Perpendicular to crank shaft axis	0.01	0.00	0.01	0.01	0.01

References

[1] Agarwal, A. K., 2007, "Bio Energy Options and Rural India," India Infrastructure report, Oxford University Press.

[2] Subramanian, K. A., Sinhgal, S. K., Saxena, M., and Singhal, S., 2005, "Utilization of Liquid Biofuels in Automotive Diesel Engines: An Indian Perspective," Biomass Bioenergy, **29**, pp. 65–72.

[3] Anon, Petroleum Statistics, Ministry of Oil & Natural Gas, Government of India, http://www.peroleum.nic.in/petsteat.pdf.

[4] Peterson, C. L., and Auld, D. L., 1991, "Technical Overview of Vegetable Oil as a Transportation Fuel," *FACT: Solid Fuel Conversion for the Transportation Sector*, Vol. 12, ASME, New York, pp. 45–54.

[5] Kowalewicz, A., and Wojtyniak, M., 2005, "Alternative Fuels and Their Application to Combustion Engines," Proc. Inst. Mech. Eng., Part D (J. Automob. Eng.), **219**, pp. 103–125.

[6] Demirba, A., 1998, "Fuel Properties and Calculation of Higher Heating Values of Vegetable Oils," Fuel, **77**(9–10), pp. 1117–1120.

[7] Barnwal, B. K., and Sharma, M. P., 2005, "Prospects of Biodiesel Production From Vegetable Oils in India," Renewable Sustainable Energy Rev., **9**(4), pp. 363–78.

[8] Srivastava, A., and Prasad, R., 2000, "Triglycerides-Based Diesel Fuels," Renewable Sustainable Energy Rev., **4**, pp. 111–133.

[9] Ma, F., and Hanna, M. A., 1999, "Biodiesel Production: A Review," Bioresour. Technol., **70**, pp. 1–15.

[10] Peterson, C. L., Wagner, G. L., and Auld, D. L., 1983, "Vegetable Oil Substitution for Diesel Fuel," Trans. ASAE, **26**, pp. 322–327.

[11] Krawczyk, T., 1996, "Biodiesel-Alternative Fuel Makes Inroads But Hurdle Remains," Informatica, **7**, pp. 801–815.

[12] Clark, S. J., Wagner, L., Schrock, M. D., and Piennaar, P. G., 1984, "Methyl and Ethyl Soybean Esters as Renewable Fuels for Diesel Engines," J. Am. Oil Chem. Soc., **61**(10), pp. 1632–1643.

[13] Murayama, T., Oh, Y., Miyamoto, N., Chikahisa, T., Takagi, N., and Itow, K., 1984, "Low Carbon Flower Buildup, Low Smoke, and Efficient Diesel Operation With Vegetable Oils by Conversion to Monoesters and Blending With Diesel Oils or Alcohols," SAE Paper No. 841161.

[14] Canakci, M., and Van Gerpen, J. H., 2001, "Comparison of Engine Performance and Emissions for Petroleum Diesel Fuel, Yellow Grease Biodiesel, and Soybean Oil Biodiesel," SAE Paper No. 016050.

[15] Rewolinski, C., and Shaffer, D. L., 1985, "Sunflower Oil Diesel Fuel: Lubrication System Contamination," J. Am. Oil Chem. Soc., **62**(7), pp. 1120–1124.

[16] Ryan, T. W., III, Dodge, L. G., and Callahan, T. J., 1984, "The Effects of Vegetable Oil Properties on Injection and Combustion in Two Different Diesel Engines," J. Am. Oil Chem. Soc., **61**(10), pp. 1610–1619.

[17] Marchetti, J. M., 2007, "Possible Methods for Bio Diesel Production," Renewable Sustainable Energy Rev., **11**(6), pp. 1300–1311.

[18] Van Gerpen, J. V., 2005, "Biodiesel Processing and Production," Fuel Process. Technol., **86**, pp. 1097–1107.

[19] Meher, L. C., 2006, "Technical Aspect of Biodiesel Production by Transesterification—A Review," Renewable Sustainable Energy Rev., **10**(3), pp. 248–268.

[20] Fukuda, H., Kondo, S., and Noda, H., 2001, "Biodiesel Fuel Production by Transesterification of Oils," J. Biosci. Bioeng., **92**(5), pp. 405–416.

[21] Schwab, A. W., Dykstra, G. J., Selkeo, E., Sorenson, S. C., and Pryde, E. H., 1988, "Diesel Fuel From Thermal Decomposition of Soybean Oil," J. Am. Oil Chem. Soc., **65**(11), pp. 1781–86.

[22] Agarwal, A. K., Bijwe, J., and Das, L. M., 2003, "Effect of Biodiesel Utilization on Wear of Vital Parts in Compression Ignition Engine," ASME J. Eng. Gas Turbines Power, **125**, pp. 604–611.

[23] Agarwal, A. K., and Das, L. M., 2001, "Biodiesel Development and Characterization for Use as a Fuel in Compression Ignition Engine," Trans. ASME: J. Eng. Gas Turbines Power, **123**, pp. 440–447.

[24] Freedman, B., Pryde, E. H., and Mounts, T. L., 1984, "Variables Affecting the Yields of Fatty Esters From Transesterified Vegetable Oils," J. Am. Oil Chem.

Downloaded 02 Jun 2010 to 171.66.16.96. Redistribution subject to ASME license or copyright; see http://www.asme.org/terms/Terms_Use.cfm

Soc., **61**, pp. 1638–1643.
[25] Vicente, G., Martinez, M., and Aracil, J., 2004, "Integrated Biodiesel Production: a Comparison of Different Homogeneous Catalysts Systems," Bioresour. Technol., **92**, pp. 297–305.
[26] Peterson, C. L., and Hustruid, T., 1998, "Carbon Cycle for Rapeseed Oil Biodiesel Fuel," Biomass Bioenergy, **14**, pp. 91–101.
[27] Devitt, M., Drysdale, D. W., MacGillivray, I., Norris, A. J., Thompson, R., and Twidell, J. W., 1983, "Biofuel for Transport: An Investigation Into the Validity of Rape Methyl Ester (RME) as an Alternative to Diesel Fuel," Int. J. Ambient Energ., **14**(4), pp. 195–218.
[28] Sinha, S., and Agarwal, A.K., 2005, "Performance Evaluation of a Biodiesel (Rice-ran Oil Methyl Ester) Fuelled Transport Diesel Engine," SAE Paper No. 2005-01-1730.
[29] Sinha, S., and Agarwal, A.K., 2006, "Combustion Characteristics of Rice Bran Oil Derived Biodiesel in a Transportation Diesel Engine," ICES Paper No. 2006-1375.
[30] Hu, J., Du, Z., Li, C., and Min, E., 2005, "Study on the Lubrication Properties of Biodiesel as Fuel Lubricity Enhancers," Fuel, **84**, pp. 1601–1606.
[31] Kinney, A. J., and Clemente, T. E., 2005, "Modifying Soybean Oil for Enhanced Performance in Biodiesel Blends," Fuel Process. Technol., **86**, pp. 1137–1147.
[32] Drown, D. C., Harper, K., and Frame, E., 2001, "Screening Vegetable Oil Alcohol Esters as Fuel Lubricity Enhancers," J. Am. Oil Chem. Soc., **78**(6), pp. 579–584.
[33] Tung, S. C., and McMillan, M. L., 2004, "Automotive Tribology Overview of Current Advances and Challenges for the Future," Tribol. Int., **37**, pp. 517–536.
[34] Gautam, M., Chitoor, K., Durbha, M., and Summers, J. C., 1999, "Effect of Diesel Soot Contaminated Oil on Engine Wear-Investigation of Novel Oil Formulations," Tribol. Int., **32**, pp. 687–699.
[35] Nagai, I., Endo, H., Nakamura, H., and Yano, H., 1983, "Soot and Valve Train Wear in Passenger Car Diesel Engines," SAE Paper No. 831757.
[36] Corso, S., and Adamo, R., 1984, "The Effect of Diesel Soot on Reactivity of Oil Additives and Valve Train Materials," SAE Paper No. 841369.
[37] Berbeizer, I., Martin, J., and Kaspa, P. H., 1986, *The Role of Carbon in Lubricated Mild Wear*, National Council for Scientific Research, France.
[38] Priest, M., and Taylor, C. M., 2000, "Automobile Engine Tribology—Approaching the Surface," Wear, **241**, pp. 193–203.
[39] Dong, W. P., Davis, E. J., Butler, D. L., and Stout, K. J., 1995, "Topographic Features of Cylinder Liners—An Application of Three-Dimensional Characterization Techniques," Tribol. Int., **28**(7), pp. 453–463.
[40] Zieba-Palus, J., 1998, "Examination of Used Motor Oils by Flame AAS for Criminalistic Purposes: A Diagnostic Study," Forensic Sci. Int., **91**, pp. 171–179.
[41] Kjer, T., 1981, "Wear Rate and Concentration of Wear Particles in Lubricating Oil," Wear, **67**, pp. 217–226.
[42] Kalam, M. A., and Masjuki, H. H., 2002, "Biodiesel From Palm Oil—An Analysis of Its Properties and Potential," Biomass Bioenergy, **23**, pp. 471–479.
[43] Agarwal, A. K., Bijwe, J., and Das, L. M., 2003, "Wear Assessment in a Biodiesel Fuelled Compression Ignition Engine," ASME J. Eng. Gas Turbines Power, **125**, pp. 820–826.
[44] Kaufman, K. R., and Ziejewski, M., 1984, "Sunflower Methyl Esters for Direct Injected Diesel Engines," Trans. ASAE, **27**, pp. 1626–1633.
[45] Fraer, R., Dinh, H., Proc, K., McCormick, R.L., Chandler, K., Buchholz, B., 2005, "Operating Experience and Teardown Analysis for Engines Operated on Biodiesel Blends (B20)," Paper No. SAE 2005-01-3641.
[46] Proc, K., Barnitt, R., Hayes, R.R., McCormick, R., Ha, L., and Fang, H., 2006, "100,000-Mile Evaluation of Transit Buses Operated on Biodiesel Blends (B20)," SAE Paper No. 2006-01-3253.
[47] Zullaikah, S., Lai, C., Vali, S. R., and Ju, Y., 2005, "A Two-Step Acid-Catalyzed Process for the Production of Biodiesel From Rice Bran Oil," Bioresour. Technol., **96**, pp. 1889–96.
[48] Sinha, S., Agarwal, A. K., and Garg, S., 2008, "Biodiesel Development From Rice Bran Oil: Transesterification Process Optimization and Fuel Characterization," Energy Convers. Manage., **49**(5), pp. 1248–1257.
[49] 1980, "Preparation for Tests and Measurement for Wear," Indian Standard Code IS: 10000, Pt. V.
[50] 1980, "Endurance Test for IC Engine, Indian Standard Code IS: 10000, Pt. IX.
[51] Staat, F., and Paul, G., 1995, "Effect of Rapeseed Oil Methyl Ester on Diesel Engine Performance, Exhaust Emissions and Long-Term Behavior—A Summary of Three Years of Experimentation," SAE Paper No. 950053.

Downloaded 02 Jun 2010 to 171.66.16.96. Redistribution subject to ASME license or copyright; see http://www.asme.org/terms/Terms_Use.cfm